# Multiple Quantum Wells for $\mathcal{PT}$-Symmetric Phononic Crystals

A. V. Poshakinskiy,[1,*] A. N. Poddubny,[1] and A. Fainstein[2]
[1]*Ioffe Institute, St. Petersburg 194021, Russia*
[2]*Centro Atomico Bariloche and Instituto Balseiro, Comisión Nacional de Energía Atómica, 8400 San Carlos de Bariloche, Río Negro, Argentina*
(Received 29 June 2016; published 23 November 2016)

We demonstrate that the parity-time symmetry for sound is realized in laser-pumped multiple-quantum-well structures. Breaking of the parity-time symmetry for the phonons with wave vectors corresponding to the Bragg condition makes the structure a highly selective acoustic wave amplifier. Single-mode distributed feedback phonon lasing is predicted for structures with realistic parameters.

DOI: 10.1103/PhysRevLett.117.224302

*Introduction.*—Parity-time ($\mathcal{PT}$) symmetry, initially proposed as a concept in quantum mechanics [1], is now being extensively studied in optics [2–4]. A $\mathcal{PT}$-symmetric optical system is the one with a dielectric permittivity distribution that is invariant under simultaneous operations of spatial inversion and complex conjugation. In such a structure, any spatial region with a loss is mirrored by a region of gain. Therefore, the processes of light absorption and amplification can be compensated, and the frequencies of eigenoptical modes can be real. An elementary $\mathcal{PT}$-symmetric structure is a pair of loss and gain cavities. It allows one to realize power oscillations [5] and tailor the nonlinear response [6,7]. In $\mathcal{PT}$-symmetric photonic crystals Bragg amplification boosts unidirectional invisibility [8–10], coherent perfect absorption [11], and single-mode lasing [12].

Recently, the concept of $\mathcal{PT}$ symmetry has been introduced into acoustics [13]. While the general ideas directly mimic optical structures, controllable sound amplification or attenuation requires completely different physical mechanisms than those for light. So far, the experimental demonstration of $\mathcal{PT}$ symmetry in a mechanical system has been limited to macroscopic pendula driven by electromagnets [14]. Another macroscopic structure based on bulk semiconductor acoustic Cherenkov amplifiers has been suggested in Ref. [15]. Promising for sound manipulation at the nanoscale are optomechanical systems [16]. Acoustic lasing [17] and optomechanically induced transparency [18] for a pair of resonators with optical $\mathcal{PT}$ symmetry, as well as the creation of nonclassical mechanical states [19] and unidirectional phonon transport [20] were predicted. The optomechanical cooling and heating effects were suggested to realize mechanical $\mathcal{PT}$ symmetry in a system of two coupled resonators [21]. However, such elements for phonon manipulation require rather sophisticated fabrication and could hardly be used for construction of complex $\mathcal{PT}$-symmetric structures with many gain and loss elements. Here we show that, due to exciton-enhanced photoelastic light-sound interaction [22], a laser-pumped quantum well (QW) with realistic parameters controllably amplifies or attenuates phonons depending on the detuning of the laser frequency from the exciton resonance. Combining QWs with positively and negatively detuned exciton frequency in the same structure we propose the technologically simple realization of $\mathcal{PT}$-symmetric phononic crystals, that, similarly to their optical counterparts, allow for new possibilities of sound manipulation.

*Sound transmission and reflection from a single QW.*—We begin with a demonstration that a single QW pumped by a laser light of the frequency close to the exciton resonance can be used for controllable phonon amplification and attenuation. The Hamiltonian describing an interaction of the longitudinal acoustic phonons with excitons in a QW reads $H = \omega_x b^\dagger b + \sum_k \Omega_k a_k^\dagger a_k + \sum_k b^\dagger b(g_k a_k + g_k^* a_k^\dagger)$, where $\omega_x$ is the QW exciton resonance frequency, $\Omega_k = s|k|$ is the phonon dispersion with $s$ being the speed of sound, $a_k$ and $b$ are the annihilation operators for the phonons and excitons, respectively, and $\hbar = 1$. The last term stands for the exciton-phonon interaction due to the deformation potential mechanism [23] with the matrix element $g_k = ik\Xi_k/\sqrt{2\rho\Omega_k S}$, where $\Xi_k = \int(\Xi_e|\psi_e(z)|^2 + \Xi_h|\psi_h(z)|^2)e^{-ikz}dz$ with $\psi_{e(h)}$ and $\Xi_{e(h)}$ being the electron (hole) confinement wave functions and deformation potential constants, respectively, $\rho$ is the mass density, and $S$ is the sample (normalization) area [24,25].

When a QW is excited by a laser of the frequency $\omega_L$ close to the exciton resonance, the coherent exciton population is created. This can be taken into account by making the substitution $b \to b_L + b$ in the Hamiltonian, where the number of laser-induced excitons is given by $|b_L|^2 = (I/\omega_L)\Gamma_0/[(\omega_L - \omega_x)^2 + \Gamma_x^2]$, $I$ is the laser power, $\Gamma_0$ and $\Gamma_x$ are the radiative and total exciton decay rates, respectively. Laser-induced excitons enhance the exciton-phonon interaction leading to the modification of the exciton spectrum [26]. This effect is described by the exciton self-energy correction $\Sigma(\omega) = |b_L|^2\sum_k |g_k|^2 D_k^{(0)}(\omega - \omega_L)$, where $D_k^{(0)}(\Omega) = 2\Omega_k/[(\Omega + i\Gamma_p)^2 - \Omega_k^2]$ is the retarded phonon Green's

 

function, and $\Gamma_p$ is the phonon decay rate due to the anharmonicity and scattering. The real and imaginary parts of the self-energy, $\Sigma(\omega_L+\Omega)=\delta\Omega(\Omega)-i\gamma(\Omega)$ read

$$\gamma(\Omega)=\frac{|b_L|^2|\Xi_k|^2\Omega}{2\rho s^3 S}, \tag{1}$$

$$\delta\Omega(\Omega)=-\frac{|b_L|^2}{\rho s^2 S}\mathrm{V.p.}\int\frac{\Omega_{k'}^2|\Xi_{k'}|^2}{\Omega_{k'}^2-\Omega^2}\frac{dk'}{2\pi}, \tag{2}$$

where $\Omega=\omega-\omega_L$ and V.p. denotes the Cauchy principal value of the integral. The real part $\delta\Omega$ describes a shift of the exciton resonance, from now on we assume that it has been already included in the exciton energy. Contrary, the imaginary part $\gamma$ leads to the pumping-induced modification of exciton lifetime that is shown below to cause phonon amplification and attenuation.

The transmission $t(\Omega)$ and reflection $r(\Omega)$ coefficients of a phonon with the frequency $\Omega$ through the pumped QW read [27],

$$t(\Omega)=1-r(\omega)=\frac{\Delta^2-(\Omega+i\Gamma_x)^2}{\Delta^2-(\Omega+i\Gamma_x)^2+2\Delta i\gamma(\Omega)}, \tag{3}$$

where $\Delta=\omega_L-\omega_x$ is the detuning of the laser from the exciton resonance. They have a pole at the frequency $\Omega\approx|\Delta|-i(\Gamma_x-\gamma\mathrm{sign}\Delta)$, that shifts towards (away from) the real axis with increasing $\gamma$ for positive (negative) laser detuning. This effect is similar to the optomechanical heating (cooling) [16], but utilizes the exciton resonance instead of cavity resonance. The maximal reflectance is achieved at the resonance frequency $\Omega_0=\sqrt{\Delta^2+\Gamma_x^2}$. Transmittance also has an extremum at $\Omega_0$, the resonant value reads $t(\Omega_0)\approx 1+(\gamma\Delta)/(\Gamma_x\Omega_0)$. Hence, the transmitted phonon is amplified if $\Delta>0$ and attenuated if $\Delta<0$.

We estimate the phonon amplification efficiency using the state-of-the-art GaAs QW parameters [22,28]. We take $\Gamma_x=0.1$ meV and consider 120 GHz phonons that overlap strongly with the QW wave functions [25], so $\Xi_k\approx$ 10 eV. Then for an exciton density realizable in experiment $|b_L|^2/S=10^{10}$ cm$^{-2}$ [29] we obtain $\gamma\approx 1$ $\mu$eV. While this corresponds only to a 1% amplification by a single QW, in structures with hundreds of QWs [30], amplification by several times is expected. Suitable methods of acoustic transmission spectroscopy are already available [31].

*Resonant $\mathcal{PT}$-symmetric phononic crystal.*—Now we consider a periodic layered structure consisting of QWs separated by barriers of width $d$, see Fig. 1. Its unit cell contains two QWs of slightly different parameters and distinct exciton resonance energies, $\omega_x^{(\pm)}=\omega_x^{(0)}\pm\delta\omega_x$. When pumped with a laser of the frequency $\omega_L$ that lies between the two resonances, a half of QWs will amplify the sound while the other half will attenuate it. We focus on the

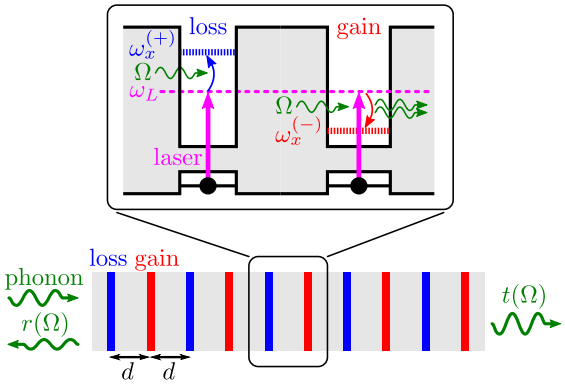


FIG. 1. Multiple-quantum-well structure with two quantum wells in the unit cell. Under laser pump, optomechanical cooling and heating takes place in the two QWs, realizing the $\mathcal{PT}$ symmetry for phonons.

case $\omega_L=\omega_x^{(0)}$, when the sound gain and loss in QWs of the two types have the same magnitude; hence, the acoustic $\mathcal{PT}$ symmetry is realized.

In order to calculate the phonon transmission coefficient through the structure we use the transfer matrix technique [32]. For each layer, a QW or a barrier, we build a $2\times 2$ transfer matrix $\hat{T}$ linking the amplitudes of the right- and left-going acoustic waves at the right layer edge with those at the left one. The matrix elements read $T_{11}=t-r^2/t$, $T_{12}=-T_{21}=r/t$, and $T_{22}=1/t$, where the transmission and reflection coefficients $t$ and $r$ are given by Eqs. (3) for a QW, while for an interwell barrier they are equal to $r=0$ and $t=e^{ikd}$, $k=(\Omega+i\Gamma_p)/s$. The transfer matrix $\hat{T}_1$ for a structure period is a product of the transfer matrices for two QWs with $\Delta=\pm\delta\omega_x$ and two barriers of width $d$. By calculating the eigenvalues $\mathrm{e}^{2iKd}$ of the matrix $\hat{T}_1$ we obtain the dispersion equation

$$\sin^2 Kd=[1-\chi^2(\Omega)]\sin^2\frac{\Omega+i\Gamma_p}{s}d, \tag{4}$$

where $\chi(\Omega)=2i\gamma\delta\omega_x/[(\Omega+i\Gamma_x)^2-\delta\omega_x^2]$. Equation (4) determines the relation between the Bloch wave vector of an acoustic wave $K$ and its frequency $\Omega$. First, we neglect the finite phonon lifetime $\Gamma_p$. If we choose $\Omega$ to be real, we will get from Eq. (4) the value of $K(\Omega)$ that has, in general, a nonzero imaginary part. The only exception is the frequency $\Omega_0=\sqrt{\delta\omega_x^2+\Gamma_x^2}$, where $\chi(\Omega_0)$ turns real, so Bloch wave vector $K(\Omega_0)$ is also real and the acoustic wave does not decay nor grow in space. The frequency $\Omega_0$ is the one where the exact $\mathcal{PT}$ symmetry for sound is realized. Because of the causality principle the exact $\mathcal{PT}$ symmetry holds only at isolated frequency points [33], in our case at the frequency $\Omega_0$. The effects discussed here are still valid in a certain vicinity of this frequency, where the deviation from $\mathcal{PT}$ symmetry is negligible.

*$\mathcal{PT}$ symmetry breaking for Bragg phonons.*—We focus on the special case when the frequency of $\mathcal{PT}$ symmetry

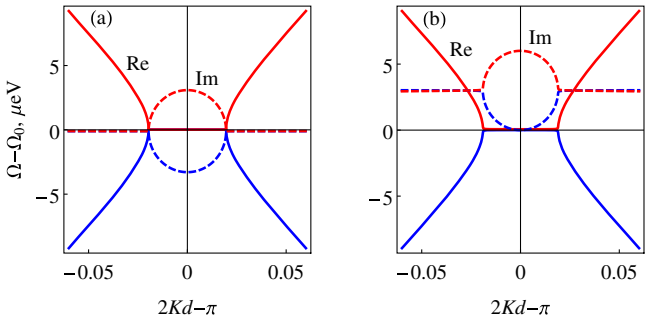


FIG. 2. Phonon dispersion for (a) the $\mathcal{PT}$-symmetric structure and (b) the structure with amplifying QWs only: dependence of the real (solid) and imaginary (dashed) parts of the phonon frequency on the phonon Bloch wave vector. Red and blue colors correspond to two phonon modes. The parameters are $\delta\omega_x = 0.5$ meV, $\Gamma_x = 0.1$ meV, $\gamma(\Omega_0) = 1$ $\mu$eV, $\Gamma_p = 0$. The interwell distance $d = 10$ nm is tuned to satisfy the Bragg condition at the frequency $\Omega_0$. The acoustic contrast is neglected.

matches the Bragg resonance condition, $\Omega_0/s = \pi/2d$. Using the Taylor expansion for Eq. (4) in the vicinity of $\Omega = \Omega_0$ and $K = \pi/2d$, we obtain the phonon dispersion

$$\Omega(K) = \Omega_0 \pm \sqrt{s^2(K-\pi/2d)^2 - G^2}, \qquad (5)$$

where $G = (s/d)\chi(\Omega_0) = 2\gamma\delta\omega_x/\pi\Gamma_x$ is the maximal mode decay or gain rate. The dispersion law of the real and imaginary parts of $\Omega(K)$ in the $\mathcal{PT}$-symmetric structure is shown in Fig. 2(a). The frequencies $\Omega(K)$ are real far from the Brillouin zone edge, $|K-\pi/2d| > G/s$, which is a consequence of $\mathcal{PT}$ symmetry. On the other hand, the frequencies of the two Bragg acoustic modes with the wave vector $|K-\pi/2d| < G/s$ have nonzero imaginary parts and are complex conjugate to each other. This can be interpreted as $\mathcal{PT}$ symmetry breaking: Indeed, the standing acoustic wave with the wave vector $K = \pi/2d$ matching the Bragg condition can either have the deformation nodes in the amplifying QWs and the antinodes in the attenuating QWs, or vice versa, resulting in the net gain or loss, respectively.

For comparison, we consider the structure where all attenuating QWs are removed, i.e., an array of amplifying QWs with the interwell distance $2d$. The sound dispersion in such structure is shown in Fig. 2(b). In that case the frequencies of all Bloch modes have the positive imaginary part. Many acoustic modes are amplified simultaneously, in contrast to the $\mathcal{PT}$-symmetric structure, amplifying only within a narrow range of wave vectors.

*Highly selective sound amplification.*—Now we consider sound transmission through the structure with $N$ periods. The transfer matrix for the structure is $\hat{T}_1^N$, and the transmission coefficient is readily expressed via the matrix element, $t_N(\Omega) = 1/[\hat{T}_1^N(\Omega)]_{22}$. Figure 3(a) shows the map of the transmittance vs the phonon frequency and the laser detuning. Whether the transmitted phonon is amplified or attenuated is determined by the laser detuning with respect to the exciton resonance energies $\omega_x^{(\pm)}$ in the two QWs forming the structure period. The areas of amplification (red color) of transmitted sound lie above either of two resonances, while the areas of attenuation (blue) lie below them. In agreement with Eq. (3), maximal amplification or attenuation occurs when $\Omega = |\omega_L - \omega_x^{(\pm)}|$. The areas of amplification and attenuation intersect at $\omega_L = \omega_x^{(0)}$, which is a signature of acoustic $\mathcal{PT}$ symmetry. The cross section of the map showing the dependence of transmittance on phonon frequency in this case is shown in Fig. 3(b): the transmittance is close to unity at all phonon frequencies except for a narrow region around the Bragg resonance. The former is the consequence of the $\mathcal{PT}$ symmetry while the latter is due to the $\mathcal{PT}$ symmetry breaking for the Bragg phonons discussed above. An analytical expression for the transmission coefficient can be obtained expressing the $N$th power of the unimodular matrix $\hat{T}^{(1)}$ via Chebyshev polynomials [34]. For frequencies in the vicinity of the Bragg resonance this gives

$$|t_N(\Omega_0+\omega)|^2 = 1 + \frac{G^2\sin^2[\sqrt{\omega^2+G^2}L/s]}{\omega^2+G^2\cos^2[\sqrt{\omega^2+G^2}L/s]}, \qquad (6)$$

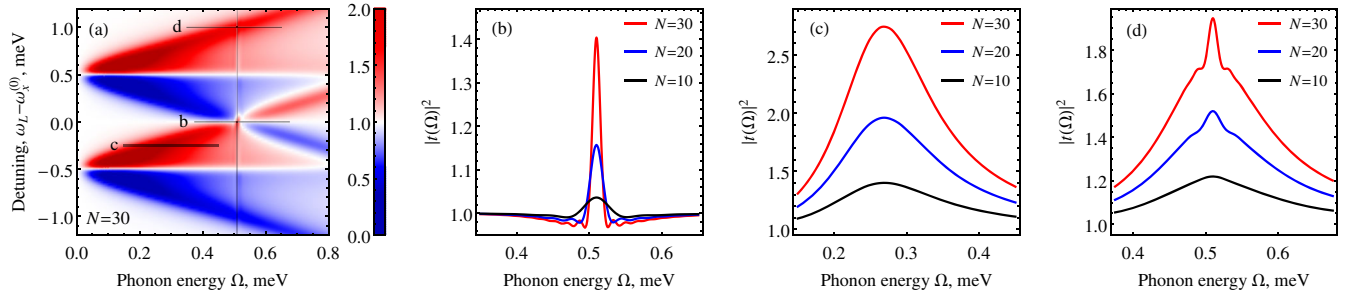


FIG. 3. (a) Map of transmittance as a function of the phonon frequency $\Omega$ and the laser energy detuning $\omega_L - \omega_x^{(0)}$ for a structure with $N = 30$ periods. Vertical line indicates the Bragg resonance frequency. (b)–(d) Cross sections of the map at fixed laser detunings, indicated by horizontal lines in panel (a). Panel (b) corresponds to the laser energy being in the middle of the exciton resonances for two types of QWs, so the $\mathcal{PT}$ symmetry is realized. The parameters are the same as those for Fig. 2.

where $L = 2dN$ is the structure length. It follows from Eq. (6) and Fig. 3(b) that the amplification bandwidth shrinks as $2\sqrt{(\Omega_0/N)^2 - G^2}$ with the structure length.

The highly selective sound amplification is a hallmark of the $\mathcal{PT}$-symmetric system. For comparison we consider the case when the laser is detuned from $\omega_x^{(0)}$ and no $\mathcal{PT}$ symmetry is present. Shown in Fig. 3(c) is the sound transmittance for the laser frequency tuned slightly above the exciton resonance $\omega_x^{(-)}$. In that case, the sound is amplified in a much broader frequency range of the width $\Gamma_x$ that does not change with the increase of the structure length. Figure 3(d) corresponds to the laser frequency tuned to satisfy the Bragg condition only at the high-energy exciton resonance, $\omega_L = \omega_x^{(+)} + \pi s/(2d)$, so the low-energy QWs are off resonant. Such structure is equivalent to that with all low-energy QWs removed. Hence, the Bloch modes are amplified in a wide range of wave vectors, even though there is some boost at the Bragg resonance; see Fig. 2(b). Concomitantly, the transmission spectrum Fig. 3(d) reveals comparatively low amplification selectivity.

*Phonon lasing transition.*—Finally, we discuss the possible application of the proposed $\mathcal{PT}$-symmetric acoustic crystal to achieve distributed feedback single-mode phonon lasing. With increase of the structure length the amplification peak grows while its width decreases, see Fig. 3(b). We plot in Fig. 4 by thick solid curves the dependence of the transmission maximum $|t(\Omega_0)|^2$ on the number of periods. The curves are calculated for the different values of $\gamma$ proportional to the pump laser intensities, and for finite phonon decay rate $\Gamma_p = 1$ $\mu$eV [35]. At low pump rate the transmission coefficient tends to zero when $N \to \infty$, see the black curve in Fig. 4. The behavior changes drastically when amplification of the Bragg mode with $K = \pi/2d$ equal to $G$, see Eq. (5), surpasses the phonon decay rate $\Gamma_p$. This takes place for $\gamma > \pi\Gamma_x\Gamma_p/2\delta\omega_x$ and means that the infinite structure becomes unstable. Consequently, the dependence of the transmission coefficient on the structure length diverges at a certain number of periods, see the blue and red curves in Fig. 4. This indicates that a complex eigenfrequency has reached the real axis and further increase of the structure length or the laser power will lead to this pole acquiring a positive imaginary part, meaning the phonon lasing transition. The critical number of periods $N_c$ found from the condition $t_{N_c}(\Omega_0) = \infty$ reads

$$N_c = \frac{1}{\pi}\frac{\Omega_0}{\sqrt{G^2 - \Gamma_p^2}}\left(\frac{\pi}{2} + \arcsin\frac{\Gamma_p}{G}\right). \tag{7}$$

Critical number decreases at high laser powers as shown in the inset of Fig. 4. The value of $\gamma = 1$ $\mu$eV corresponds approximately to the pump laser intensity 1 mW per $\mu m^2$ cross section. Such small power densities are readily accessible, evidencing the high efficiency of the proposed approach.

Even if the structure itself is amplifying but not yet lasing, one can attain the lasing by embedding it into an acoustic cavity [36–38] or placing it near an interface with vacuum. Assuming perfect phonon reflection from the interface, and tuning the distance from the interface to the first amplifying QW to $\lambda/4$, we will get lasing as soon as $|r(\Omega_0)| > 1$. Shown in Fig. 4 by thin curves is the dependence of the reflection coefficient on the structure length. One can see that $|r(\Omega_0)|$ reaches unity for twice shorter than critical structure. Indeed, the reflection from the interface makes the structure effectively twice longer, consequently reducing the critical lasing length by the factor of 2.

After 60 years of existence of the lasers their acoustic counterparts have not reached a technological stage, notwithstanding the efforts involved and the promising possible applications that range from nm-resolution echography and microscopy [39] to THz-frequency manipulation of optical signals [40], spins, or other excitations in solids [41]. A proved physical mechanism for efficient phonon stimulation is self-oscillations in optomechanical resonators [16,42,43]. However, such systems require rather sophisticated fabrication, and phonon extraction remains a critical unresolved issue. Phonon amplification and stimulation [44–46] based on unipolar carrier transport in semiconductor superlattices, conceptually similar to quantum cascade lasers [47], have been also experimentally demonstrated. Despite the mature fabrication technology of these structures, the observed efficiency is very low, hampering their applications. We propose the laser-pumped quantum wells with red- and blue-detuned exciton

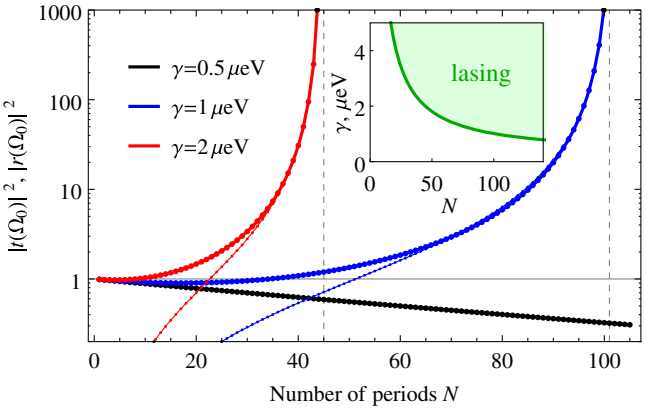


FIG. 4. Dependence of the resonant sound transmission (thick) and reflection (thin) coefficients on the number of periods in the structure $N$ plotted for different powers of pump laser, characterized by the value of $\gamma$. Vertical dashed lines indicate the critical number of periods $N_c$ when acoustic lasing transition occurs. Inset: Dependence of the critical value of $\gamma$ on the number of periods $N$. Calculation is made for $\Gamma_p = 1$ $\mu$eV and other parameters are the same as for Fig. 2.

resonances combined in the same structure for controllable amplification and attenuation of phonons at the nanoscale. A violation of $\mathcal{PT}$ symmetry for very specific phonon modes leads to a very narrow linewidth for stimulation, allowing for single mode lasing. The very small power densities predicted to attain the phonon instabilities for realistic parameters evidence the high efficiency of our approach. Moreover, multiple quantum well structures form an established and rugged platform successfully used for many optoelectronic applications. Complex structures with many gain and loss elements can be monolithically grown with optoelectronic components, avoiding phonon interfacing issues [48]. Integrated optomechanical and optoelectronic performance could thus be envisaged for the demonstration of novel physical phenomena and applications involving $\mathcal{PT}$-symmetry concepts.

A. V. P. and A. N. P. acknowledge support by Russian President Grants No. MK-8500.2016.2 and No. SP-2912.2016.5, Russian Foundation for Basic Research Grants No. 14-29-07243-OFI and No. 16-02-00204 A, and the Foundation "Dynasty." A. F. acknowledges support by ANPCyT Grants No. PICT 2012-1661 and No. 2013-2047.

*poshakinskiy@mail.ioffe.ru

[1] C. M. Bender and S. Boettcher, Real Spectra in Non-Hermitian Hamiltonians Having $\mathcal{PT}$ Symmetry, Phys. Rev. Lett. **80**, 5243 (1998).

[2] A. A. Zyablovsky, A. P. Vinogradov, A. A. Pukhov, A. V. Dorofeenko, and A. A. Lisyansky, PT-symmetry in optics, Usp. Fiz. Nauk **184**, 1177 (2014).

[3] S. V. Suchkov, A. A. Sukhorukov, J. Huang, S. V. Dmitriev, C. Lee, and Y. S. Kivshar, Nonlinear switching and solitons in PT-symmetric photonic systems, Laser Photonics Rev. **10**, 177 (2016).

[4] V. V. Konotop, J. Yang, and D. A. Zezyulin, Nonlinear waves in $\mathcal{PT}$-symmetric systems, Rev. Mod. Phys. **88**, 035002 (2016).

[5] C. E. Rüter, K. G. Makris, R. El-Ganainy, D. N. Christodoulides, M. Segev, and D. Kip, Observation of parity–time symmetry in optics, Nat. Phys. **6**, 192 (2010).

[6] H. Hodaei, M.-A. Miri, M. Heinrich, D. N. Christodoulides, and M. Khajavikhan, Parity-time-symmetric microring lasers, Science **346**, 975 (2014).

[7] B. Peng, Ş. K. Özdemir, F. Lei, F. Monifi, M. Gianfreda, G. L. Long, S. Fan, F. Nori, C. M. Bender, and L. Yang, Parity–time-symmetric whispering-gallery microcavities, Nat. Phys. **10**, 394 (2014).

[8] Z. Lin, H. Ramezani, T. Eichelkraut, T. Kottos, H. Cao, and D. N. Christodoulides, Unidirectional Invisibility Induced by $\mathcal{PT}$-Symmetric Periodic Structures, Phys. Rev. Lett. **106**, 213901 (2011).

[9] L. Feng, Y.-L. Xu, W. S. Fegadolli, M.-H. Lu, J. E. B. Oliveira, V. R. Almeida, Y.-F. Chen, and A. Scherer, Experimental demonstration of a unidirectional reflectionless parity-time metamaterial at optical frequencies, Nat. Mater. **12**, 108 (2012).

[10] A. Regensburger, C. Bersch, M.-A. Miri, G. Onishchukov, D. N. Christodoulides, and U. Peschel, Parity–time synthetic photonic lattices, Nature (London) **488**, 167 (2012).

[11] Y. D. Chong, L. Ge, and A. D. Stone, $\mathcal{PT}$-Symmetry Breaking and Laser-Absorber Modes in Optical Scattering Systems, Phys. Rev. Lett. **106**, 093902 (2011).

[12] L. Feng, Z. J. Wong, R.-M. Ma, Y. Wang, and X. Zhang, Single-mode laser by parity-time symmetry breaking, Science **346**, 972 (2014).

[13] X. Zhu, H. Ramezani, C. Shi, J. Zhu, and X. Zhang, $\mathcal{PT}$-Symmetric Acoustics, Phys. Rev. X **4**, 031042 (2014).

[14] C. M. Bender, B. K. Berntson, D. Parker, and E. Samuel, Observation of PT phase transition in a simple mechanical system, Am. J. Phys. **81**, 173 (2013).

[15] J. Christensen, M. Willatzen, V. R. Velasco, and M.-H. Lu, Parity-Time Synthetic Phononic Media, Phys. Rev. Lett. **116**, 207601 (2016).

[16] M. Aspelmeyer, T. J. Kippenberg, and F. Marquardt, Cavity optomechanics, Rev. Mod. Phys. **86**, 1391 (2014).

[17] H. Jing, S. K. Özdemir, X.-Y. Lü, J. Zhang, L. Yang, and F. Nori, $\mathcal{PT}$-Symmetric Phonon Laser, Phys. Rev. Lett. **113**, 053604 (2014).

[18] H. Jing, Ş. K. Özdemir, Z. Geng, J. Zhang, X.-Y. Lü, B. Peng, L. Yang, and F. Nori, Optomechanically-induced transparency in parity-time-symmetric microresonators, Sci. Rep. **5**, 9663 (2015).

[19] X.-Y. Lü, Y. Wu, J. R. Johansson, H. Jing, J. Zhang, and F. Nori, Squeezed Optomechanics with Phase-Matched Amplification and Dissipation, Phys. Rev. Lett. **114**, 093602 (2015).

[20] J. Zhang, B. Peng, Ş. K. Özdemir, Y.-x. Liu, H. Jing, X.-y. Lü, Y.-l. Liu, L. Yang, and F. Nori, Giant nonlinearity via breaking parity-time symmetry: A route to low-threshold phonon diodes, Phys. Rev. B **92**, 115407 (2015).

[21] X.-W. Xu, Y.-x. Liu, C.-P. Sun, and Y. Li, Mechanical $\mathcal{PT}$ symmetry in coupled optomechanical systems, Phys. Rev. A **92**, 013852 (2015).

[22] B. Jusserand, A. N. Poddubny, A. V. Poshakinskiy, A. Fainstein, and A. Lemaitre, Polariton Resonances for Ultrastrong Coupling Cavity Optomechanics in GaAs/AlAs Multiple Quantum Wells, Phys. Rev. Lett. **115**, 267402 (2015).

[23] P. Y. Yu and M. Cardona, Fundamentals of Semiconductors: Physics and Materials Properties, *Graduate texts in physics* (Springer, New York, 2010).

[24] B. Jusserand, Selective resonant interaction between confined excitons and folded acoustic phonons in GaAs/AlAs multi-quantum wells, Appl. Phys. Lett. **103**, 093112 (2013).

[25] A. N. Poddubny, A. V. Poshakinskiy, B. Jusserand, and A. Lemaître, Resonant Brillouin scattering of excitonic polaritons in multiple-quantum-well structures, Phys. Rev. B **89**, 235313 (2014).

[26] L. V. Keldysh and S. G. Tikhodeev, High-intensity polariton wave near the stimulated scattering threshold, Zh. Eksp. Teor. Fiz. **90**, 1852 (1986) [Sov. Phys. JETP **63**, 1086 (1986)].

[27] See Supplemental Material at http://link.aps.org/supplemental/10.1103/PhysRevLett.117.224302 for the

derivation of the reflection and transmission coefficients by means of the Keldysh diagram technique.

[28] A. V. Trifonov, S. N. Korotan, A. S. Kurdyubov, I. Ya. Gerlovin, I. V. Ignatiev, Yu. P. Efimov, S. A. Eliseev, V. V. Petrov, Yu. K. Dolgikh, V. V. Ovsyankin, and A. V. Kavokin, Nontrivial relaxation dynamics of excitons in high-quality InGaAs/GaAs quantum wells, Phys. Rev. B **91**, 115307 (2015).

[29] A. Kavokin, J. J. Baumberg, G. Malpuech, and F. P. Laussy, *Microcavities* (Clarendon Press, Oxford, 2006).

[30] J. P. Prineas, C. Ell, E. S. Lee, G. Khitrova, H. M. Gibbs, and S. W. Koch, Exciton-polariton eigenmodes in light-coupled $In_{0.04}Ga_{0.96}As/GaAs$ semiconductor multiple-quantum-well periodic structures, Phys. Rev. B **61**, 13863 (2000).

[31] A. Huynh, N. D. Lanzillotti-Kimura, B. Jusserand, B. Perrin, A. Fainstein, M. F. Pascual-Winter, E. Peronne, and A. Lemaître, Subterahertz Phonon Dynamics in Acoustic Nanocavities, Phys. Rev. Lett. **97**, 115502 (2006).

[32] E. L. Ivchenko, *Optical Spectroscopy of Semiconductor Nanostructures* (Alpha Science International, Harrow, 2005).

[33] A. A. Zyablovsky, A. P. Vinogradov, A. V. Dorofeenko, A. A. Pukhov, and A. A. Lisyansky, Causality and phase transitions in $\mathcal{PT}$-symmetric optical systems, Phys. Rev. A **89**, 033808 (2014).

[34] Max Born and Emil Wolf, *Principles of Optics: Electromagnetic Theory of Propagation, Interference and Diffraction of Light* (Cambridge University Press, Cambridge, England, 1999).

[35] G. Rozas, M. F. Pascual Winter, B. Jusserand, A. Fainstein, B. Perrin, E. Semenova, and A. Lemaître, Lifetime of THz Acoustic Nanocavity Modes, Phys. Rev. Lett. **102**, 015502 (2009).

[36] M. Trigo, A. Bruchhausen, A. Fainstein, B. Jusserand, and V. Thierry-Mieg, Confinement of Acoustical Vibrations in a Semiconductor Planar Phonon Cavity, Phys. Rev. Lett. **89**, 227402 (2002).

[37] N. D. Lanzillotti-Kimura, A. Fainstein, A. Huynh, B. Perrin, B. Jusserand, A. Miard, and A. Lemaître, Coherent Generation of Acoustic Phonons in an Optical Microcavity, Phys. Rev. Lett. **99**, 217405 (2007).

[38] A. Fainstein, N. D. Lanzillotti-Kimura, B. Jusserand, and B. Perrin, Strong Optical-Mechanical Coupling in a Vertical GaAs/AlAs Microcavity for Subterahertz Phonons and Near-Infrared Light, Phys. Rev. Lett. **110**, 037403 (2013).

[39] T. Dehoux, M. A. Ghanem, O. F. Zouani, J.-M. Rampnoux, Y. Guillet, S. Dilhaire, M.-C. Durrieu, and B. Audoin, All-optical broadband ultrasonography of single cells, Sci. Rep. **5**, 8650 (2015).

[40] M. M. de Lima. Jr., R. Hey, P. V. Santos, and A. Cantarero, Phonon-Induced Optical Superlattice, Phys. Rev. Lett. **94**, 126805 (2005).

[41] A. V. Scherbakov, A. S. Salasyuk, A. V. Akimov, X. Liu, M. Bombeck, C. Brüggemann, D. R. Yakovlev, V. F. Sapega, J. K. Furdyna, and M. Bayer, Coherent Magnetization Precession in Ferromagnetic (Ga, Mn)As Induced by Picosecond Acoustic Pulses, Phys. Rev. Lett. **105**, 117204 (2010).

[42] T. J. Kippenberg, H. Rokhsari, T. Carmon, A. Scherer, and K. J. Vahala, Analysis of Radiation-Pressure Induced Mechanical Oscillation of an Optical Microcavity, Phys. Rev. Lett. **95**, 033901 (2005).

[43] I. S. Grudinin, H. Lee, O. Painter, and K. J. Vahala, Phonon Laser Action in a Tunable Two-Level System, Phys. Rev. Lett. **104**, 083901 (2010).

[44] A. J. Kent, R. N. Kini, N. M. Stanton, M. Henini, B. A. Glavin, V. A. Kochelap, and T. L. Linnik, Acoustic Phonon Emission from a Weakly Coupled Superlattice under Vertical Electron Transport: Observation of Phonon Resonance, Phys. Rev. Lett. **96**, 215504 (2006).

[45] R. P. Beardsley, A. V. Akimov, M. Henini, and A. J. Kent, Coherent Terahertz Sound Amplification and Spectral Line Narrowing in a Stark Ladder Superlattice, Phys. Rev. Lett. **104**, 085501 (2010).

[46] W. Maryam, A. V. Akimov, R. P. Campion, and A. J. Kent, Dynamics of a vertical cavity quantum cascade phonon laser structure, Nat. Commun. **4**, 2184 (2013).

[47] J. Faist, F. Capasso, D. L. Sivco, C. Sirtori, A. L. Hutchinson, and A. Y. Cho, Quantum Cascade Laser, Science **264**, 553 (1994).

[48] M. S. Muha, A. A. Moulthrop, G. C. Kozlowski, and B. Hadimioglu, Acoustic microscopy at 15.3 GHz in pressurized superfluid helium, Appl. Phys. Lett. **56**, 1019 (1990).